*Journal of Zhejiang University-SCIENCE B (Biomedicine & Biotechnology)* *2024 25(4):341-353*
www.jzus.zju.edu.cn; www.springer.com/journal/11585
E-mail: jzus_b@zju.edu.cn

**Research Article**

https://doi.org/10.1631/jzus.B2300033

Check for updates

# ELABELA-derived peptide ELA13 attenuates kidney fibrosis by inhibiting the Smad and ERK signaling pathways

Zhibin YAN[1*], Ying SHI[2*], Runling YANG[3], Jijun XUE[2], Caiyun FU[1,3✉]

[1]*Zhejiang Provincial Key Laboratory of Silkworm Bioreactor and Biomedicine, College of Life Sciences and Medicine, Zhejiang Sci-Tech University, Hangzhou 310018, China*
[2]*State Key Laboratory of Applied Organic Chemistry, College of Chemistry and Chemical Engineering, Lanzhou University, Lanzhou 730000, China*
[3]*Key Laboratory of Preclinical Study for New Drugs of Gansu Province, School of Basic Medical Sciences & Research Unit of Peptide Science, Chinese Academy of Medical Sciences, 2019RU066, Lanzhou University, Lanzhou 730000, China*

**Abstract:** Kidney fibrosis is an inevitable result of various chronic kidney diseases (CKDs) and significantly contributes to end-stage renal failure. Currently, there is no specific treatment available for renal fibrosis. ELA13 (amino acid sequence: RRCMPLHSRVPFP) is a conserved region of ELABELA in all vertebrates; however, its biological activity has been very little studied. In the present study, we evaluated the therapeutic effect of ELA13 on transforming growth factor-β1 (TGF-β1)-treated NRK-52E cells and unilateral ureteral occlusion (UUO) mice. Our results demonstrated that ELA13 could improve renal function by reducing creatinine and urea nitrogen content in serum, and reduce the expression of fibrosis biomarkers confirmed by Masson staining, immunohistochemistry, real-time polymerase chain reaction (RT-PCR), and western blot. Inflammation biomarkers were increased after UUO and decreased by administration of ELA13. Furthermore, we found that the levels of essential molecules in the mothers against decapentaplegic (Smad) and extracellular signal-regulated kinase (ERK) pathways were reduced by ELA13 treatment in vivo and in vitro. In conclusion, ELA13 protected against kidney fibrosis through inhibiting the Smad and ERK signaling pathways and could thus be a promising candidate for anti-renal fibrosis treatment.

**Key words:** ELA13; Kidney fibrosis; Inflammation; Smad; Extracellular signal-regulated kinase (ERK)

## 1 Introduction

Renal fibrosis is the common pathway of various chronic nephropathies and is characterized by excess deposition of extracellular matrix (ECM) in kidney tissues (Harris and Neilson, 2006; Zeisberg and Neilson, 2010). In China, the prevalence of chronic kidney diseases (CKDs) in adults over the age of 18 years has reached 10.8% (Zhuang et al., 2022), and CKDs are also a global concern (Akter et al., 2021). Once CKDs progress, renal interstitial fibroblasts are activated, ECM accumulates, and extensive scar tissue forms in renal tissue, eventually leading to the destruction of renal parenchymal cells and end-stage renal failure, which have high risks of morbidity and mortality (El-Ghoul et al., 2009; Romagnani and Kalluri, 2009; Kanda et al., 2017; Rahman MH et al., 2022). So far, however, no specific treatment has become available to prevent CKDs or improve kidney fibrosis. Therefore, it is of immediate importance to develop anti-fibrotic agents to slow down kidney fibrosis (Rahman MA et al., 2022).

The mechanisms of renal fibrosis have been widely investigated. Fibroblasts and myofibroblasts are considered to be two vital effector cells related to fibrogenesis processes such as ECM synthesis and deposition (el Agha et al., 2017). Inflammatory reaction also plays a vital role in triggering kidney fibrosis by releasing inflammatory cytokines (Meng et al., 2014; Yan et al., 2022). In addition, numerous studies indicate that the progression of renal fibrosis is linked to many signaling pathways, including mitogen-activated protein kinases (MAPKs) (Jiang et al., 2017) and the transforming growth factor-β1 (TGF-β1)/mothers against decapentaplegic (Smad) (Lan, 2011), Wnt/β-catenin

✉ Caiyun FU, fucy03@zstu.edu.cn
* The two authors contributed equally to this work
Caiyun FU, https://orcid.org/0000-0003-4090-885X

Received Jan. 11, 2023; Revision accepted Apr. 13, 2023;
Crosschecked Mar. 26, 2024

(Li et al., 2017), angiogenesis (Tanaka et al., 2015), cellular apoptosis (Ding et al., 2014), and hypoxia pathways (Tanaka et al., 2015). TGF-β, the crucial profibrotic cytokine, induces an imbalance in ECM regulation and activation of resident myofibroblasts (López-Hernández and López-Novoa, 2012). At present, several TGF-β inhibitors are in different stages of clinical investigation, for example AP12009 (Korpal and Kang, 2010) and LY2157299 (Kovacs et al., 2015). Members of the Smads family are requisite intermediaries of canonical TGF-β pathways (Lan, 2011; Zhang et al., 2015). Phosphorylated (p-) Smads proteins translocate into the nucleus and regulate expression of downstream genes (Meng et al., 2015). Ji et al. (2018) showed the inhibition of fibrosis, apoptosis, and inflammation by a specific inhibitor of Smad3 in mouse unilateral ureteral obstruction (UUO) kidneys. Activation of extracellular signal-regulated kinase (ERK), one of the MAPKs, regulates many cellular biological processes involved in kidney fibrogenesis, such as apoptosis, cell proliferation, epithelial-to-mesenchymal transition (EMT), and ECM deposition (Nutter et al., 2015).

ELABELA, another recently discovered ligand of the apelin receptor (Aplnr/APJ), encodes a conserved C-terminal mature peptide hormone of 54 or 32 amino acids. In recent years, substantial evidence has shown the importance of the apelinergic system (Reichman-Fried and Raz, 2014). Apelin and APJ are widely distributed in various tissues of the body (Wang et al., 2015), while ELABELA is mainly distributed in the kidney in adults (Schreiber et al., 2016); this also suggests the importance of ELABELA for renal function. Recent studies have illustrated that ELA32 and ELA11 have anti-inflammatory, anti-apoptotic, and anti-fibrotic functions after ischemia-reperfusion injury (Chen et al., 2017). ELA13 (amino acid sequence: RRCMPLHSRVPFP) is a conserved region of ELABELA in all vertebrates and its activity has not been fully identified. Therefore, we designed this study to investigate the beneficial effects and potential mechanisms of ELA13 in UUO-induced renal fibrosis.

## 2 Materials and methods

### 2.1 Peptide synthesis

Based on the traditional solid-phase peptide synthesis method, we synthesized ELA13 with the Fmoc strategy, and chose 2-chlorotrityl chloride resin (0.98 mmol/g, GL Biochem, Shanghai, China) as the solid phase carrier. Briefly, each Fmoc-protected amino acid (3 equiv, GL Biochem) was coupled using *O*-benzotriazole-*N*,*N*,*N*',*N*'-tetramethyl-uronium-hexafluorophosphate (HBTU; 3 equiv, GL Biochem) as a coupling reagent, 1-hydroxybenzotriazole (HOBT; 3 equiv, GL Biochem) as a racemic inhibitor, and *N*,*N*-diisopropylethylamine (DIPEA; 6 equiv, Energy Chemical, Shanghai, China) as a base catalyst. We dissolved the mixture with *N*,*N*-dimethylformamide (DMF; 5 mL, Innochem, Beijing, China) and agitated it for 60–120 min at room temperature. After each step of the coupling reaction, the *N*-Fmoc group was detached with 20% (volume fraction) piperidine for 20 min. The resin was washed using DMF after each coupling and cleavage reaction. ELA13 peptides were dissolved in a mixture consisting of trifluoroacetic acid (TFA)/$H_2O$/triisopropylsilane (TIPS)/1,2-ethane dithiol (EDT) (37/1/1/1, volume ratio) to separate them from the resin, and agitated for 4 h at room temperature. We collected the mixture in a round-bottomed flask, and then washed the resin with TFA three times and collected the TFA solution in the previous container. The mixture was concentrated by rotary evaporation; the residuum was added to ether and centrifuged at 3500 r/min for 10 min to obtain crude peptide. Preparative high-performance liquid chromatography (HPLC) was used to purify the crude peptide, with the volume ration of mobile phase acetonitrile increased from 10% to 50% in 80 min. The solution was collected when the purpose peak appeared. After confirming the results with a liquid chromatograph-mass spectrometer (LC-MS), we dried the objective peptide in a freeze dryer.

### 2.2 Animal experiment

Male C57BL/6J mice, weighing 20–25 g (six weeks old), were purchased from the Shanghai Slac Laboratory Animal Co., Ltd., China. The mice were kept in an experimental environment that alternated between day and night for 12 h, and had free access to food and water. One week after adaptation, the mice were subjected to unilateral ureteral ligation or a sham operation after anesthetization by intraperitoneal injection of trichloroacetaldehyde hydrate (Macklin, Shanghai, China). On the second day after the operation was completed, the mice were randomly divided into four groups (six mice per group): a sham group,

sham+ELA13 group, UUO group, and UUO+ELA13 group. The sham+ELA13 group and the UUO+ELA13 group were subcutaneously injected with ELA13 (1.2 μmol/kg) twice a day (10:00 and 18:00) (Chen et al., 2017; Zhang et al., 2019); the remaining two groups were injected with equivalent phosphate-buffered saline (PBS) as control. Fourteen days later, we collected blood from the retroorbital plexus and removed the kidneys after anesthetization. The blood was used to measure renal function. The operated kidney was divided into two halves, one of which was immersed in Formalin solution and the other stored in the refrigerator at −80 ℃.

### 2.3 Histopathological staining

The renal tissue was embedded in paraffin and then cut into 4-μm sections. Following the instructions, we performed hematoxylin and eosin (H&E) and Masson staining of the tissue sections. In brief, the sections were heated in the oven at 65 ℃ for 1.5 h, deparaffinized in xylene, hydrated with ethanol solution, stained with hematoxylin at room temperature for 5 min, differentiated with 1% (volume fraction) hydrochloric acid ethanol for 1 s, tap-water washed, and recolored. One batch of slides was dyed with eosin at room temperature for 5 min; the other batch was stained with Ponceau S for 10 min, immersed in 1% (volume fraction) phosphomolybdic acid for 5 min, and then put directly into 2% (0.02 g/mL) aniline blue solution for 10 min. After the two batches of slices were dyed and washed with tap water, we used a gradient concentration of alcohol solution to dehydrate them, and soaked them in the xylene for 10 min to hyalinize the tissue. Finally, we sealed them with neutral gum. The colored area was observed and photographed, and measured using ImageJ software. For statistical analysis of Masson staining, we selected 30 fields in each group of sections, analyzed the proportion of target protein in each field with ImageJ software, and analyzed the data.

### 2.4 Immunohistochemistry staining

Immunohistochemistry staining was performed with a standard immunostaining protocol. In short, paraffin-embedded kidney sections were deparaffinized in the oven at 65 ℃ for 2 h and autoclaved for 15 min at 121 ℃ in 10 mmol/L citrate buffer (pH 6.0) to retrieve antigens, and endogenous peroxidase was blocked with 3% (volume fraction) hydrogen peroxide, followed by incubation with 10% (0.1 g/mL) bovine serum albumin (BSA) in PBS to block nonspecific binding of antibodies. Then, the slices of pretreated kidneys were incubated with the following primary antibodies overnight in the 4 ℃ refrigerator: anti-Collagen I (1:300 (volume ratio, the same below); Boster, China), anti-fibronectin (1:300; Boster), anti-α-smooth muscle actin (anti-α-SMA; 1:200; Abcam, Cambridge, UK), and anti-cluster of differentiation 68 (anti-CD68; 1:300; Boster). Next, we took the slices out of the refrigerator and added secondary antibodies; we then incubated them at 37 ℃ for 1 h. After washing with PBS, dehydrating, and air-drying slices, we detected immune complexes with diaminobenzidine (DAB, Sigma-Aldrich, USA). Finally, these slides were photographed and the colored area was calculated using ImageJ software, with the same statistical method as described above.

### 2.5 RT-PCR

The total RNA in the tissue was extracted with TRIzol reagent (Invitrogen, Carlsbad, USA) as follows: we added 1 mL of TRIzol reagent into 30 mg kidney tissue, and used a grinding apparatus to crush the tissue. Then we added 500 μL of chloroform, shook and mixed well, centrifuged the mixture at 12 000 r/min for 15 min, and put about 400 μL of the supernatant into a new centrifugal tube. Next, we added 1 mL of isopropanol to the supernatant, shook it gently and set it aside for 10 min, centrifuged it for 10 min, discarded the supernatant, added 75% (volume fraction) ethanol to wash the remaining isopropanol, absorbed the ethanol, and dried the white precipitate, which is the RNA. Then, we used a TransScript one-step genomic DNA (gDNA) removal and complementary DNA (cDNA) synthesis kit (TransGen Biotech, Beijing, China) to reverse transcription. Based on the instructions for the TransStart Top Green quantitative polymerase chain reaction (qPCR) kit (TransGen Biotech, Beijing, China), we used real-time PCR (RT-PCR) to detect the expression of the target gene. The primer sequences of target genes we used are shown in Table 1.

### 2.6 Immunoblotting

The proteins in the kidney tissue (about 30 mg) were extracted with radio immunoprecipitation assay (RIPA) lysis buffer which contained 1% (0.01 g/mL) phenylmethylsulfonyl fluoride (PMSF). We used BCA

**Table 1 Sequences of RT-PCR primers used in this study**

| Gene | Primer sequence (5'→3') |
|---|---|
| *Collagen I* | Forward: GCTCCTCTTAGGGGCCACT |
| | Reverse: CCACGTCTCACCATTGGGG |
| *Fibronectin* | Forward: GCTCAGCAAATCGTGCAGC |
| | Reverse: CTAGGTAGGTCCGTTCCCACT |
| *α-SMA* | Forward: GTCCCAGACATCAGGGAGTAA |
| | Reverse: TCGGATACTTCAGCGTCAGGA |
| *TGF-β1* | Forward: TCTGCATTGCACTTATGCTGA |
| | Reverse: AAAGGGCGATCTAGTGATGGA |
| *IL-1β* | Forward: GCAACTGTTCCTGAACTCAACT |
| | Reverse: ATCTTTTGGGGTCCGTCAACT |
| *IL-6* | Forward: TAGTCCTTCCTACCCCAATTTCC |
| | Reverse: TTGGTCCTTAGCCACTCCTTC |
| *MCP-1* | Forward: TTAAAAACCTGGATCGGAACCAA |
| | Reverse: GCATTAGCTTCAGATTTACGGGT |
| *GAPDH* | Forward: AGGTCGGTGTGAACGGATTTG |
| | Reverse: TGTAGACCATGTAGTTGAGGTCA |

RT-PCR: real-time polymerase chain reaction; α-SMA: α-smooth muscle actin; TGF-β1: transforming growth factor-β1; IL-1β: interleukin-1β; IL-6: interleukin-6; MCP-1: monocyte chemotactic protein-1; GAPDH: glyceraldehyde-3-phosphate dehydrogenase.

protein assay kit (Thermo Fisher Scientific, Waltham, USA) to detect the concentration of the protein. We added the loading buffer to concentration-regulated samples and heated them to deactivate the protein. Sodium dodecyl sulfate-polyacrylamide gel electrophoresis (SDS-PAGE) was used to separate protein at a constant current voltage of 120 V. Then, the protein was transferred to an Immobilon®-PSQ transfer membrane (Merck Millipore, Germany) at 250 mA for 120 min and the membranes were washed with Tris-buffered saline with Tween (TBST). Non-fat milk (0.05 g/mL) was used to block nonspecific proteins for 1 h, and the membrane was incubated with the following primary antibodies overnight in the refrigerator: anti-Collagen I (1:500 (volume ratio, the same below); Boster), anti-fibronectin (1:500; Boster), anti-α-SMA (1:1000; Abcam), anti-TGF-β1 (1:1000; Abcam), anti-tumor necrosis factor-α (anti-TNF-α; 1:1000; Santa Cruz, USA), anti-monocyte chemotactic protein-1 (anti-MCP-1; 1:1000; Santa Cruz), anti-interleukin-6 (anti-IL-6; 1:1000; Santa Cruz), anti-interleukin-1β (anti-IL-1β; 1:1000; Santa Cruz), anti-CD68 (1:500; Boster), anti-p-Smad2/3 (1:1000, Cell Signaling Technology, USA), anti-Smad2/3 (1:1000; Santa Cruz), anti-p-ERK1/2 (1:1000; Santa Cruz), anti-ERK1/2 (1:1000, Cell Signaling Technology), and anti-glyceraldehyde-3-phosphate dehydrogenase (anti-GAPDH; 1:1000; Santa Cruz). Based on the principle of chemical substrate luminescence, we used horseradish peroxidase (HRP)-labeled antibody to incubate membranes at room temperature for 1 h, and detected luminescence intensity with a Tanon-5200 Multi instrument (Tanon, Shanghai, China). The strip grayscale was calculated with ImageJ software.

### 2.7 Cell culture

Tubular epithelial cells (NRK-52E) were cultured in Dulbecco's modified Eagle's medium (DMEM; Misencell, Jinhua, China) with 5.5 mmol/L glucose, 10% (0.1 g/mL) fetal bovine serum (Misencell), and 1% (volume fraction) penicillin-streptomycin in an incubator set at 37 °C and 5% $CO_2$. To test the effect of ELA13 on the fibrotic cell model induced by recombinant human TGF-β1 (Peprotech, New Jersey, USA), we cultured NRK-52E cells in a six-well culture plate with $1\times10^4$ cells per well; after a day of cultivation, we starved the cells with the serum-free medium for one night. The cells were randomly divided into a control group (DMEM), an administration group (ELA13, 50 μmol/L), a model group (TGF-β1, 5 ng/mL), and a treatment group (ELA13, 50 μmol/L; TGF-β1, 5 ng/mL), and cultured for 48 h at 37 °C. To confirm the involvement of Smad and ERK signaling in anti-fibrotic effects of ELA13, we pretreated all the cells for 1 h with asiaticoside (50 μmol/L) and U0126 (50 μmol/L), which are inhibitors of SMAD and ERK.

### 2.8 Cell viability

The cytotoxicity of ELA13 was detected with a cell counting kit-8 (CCK-8; Yeasen, Shanghai, China). To each well of the 96-well plate we added 100 μL of a cell suspension containing 2000 cells. Series concentrations of ELA13 were prepared to change the medium: 100, 50, 25, 12.5, 6.25, and 0 μmol/L. For 2 d in a row, we added 10 μL CCK-8 solution and incubated the suspension at 37 °C for 2–4 h. Finally, we measured the absorbance at a wavelength of 450 nm.

### 2.9 Statistical analyses

All results were expressed as mean±standard deviation (SD). Images were generated using GraphPad Prism 9.0 (San Diego, USA). The differences between groups were statistically analyzed using one-way analysis of variance (ANOVA) followed by Tukey-Kramer

as a post-hoc test. Differences were considered statistically significant when $P<0.05$.

## 3 Results

### 3.1 Effects of ELA13 on expression of renal fibrosis markers in vitro

We first detected the safe concentration of ELA13 in NRK-52E cells by CCK-8 assay. The results demonstrated that ELA13 had no significantly effect on cell viability within 100 μmol/L (Fig. 1a). Then we detected the expression of fibrosis markers Collagen I, fibronectin, and α-SMA in TGF-β1-induced NRK-52E by western blot. As shown in Figs. 1b–1e, the expression levels of fibrosis markers increased after induction of TGF-β1 but decreased obviously after treatment with ELA13. These results demonstrated that ELA13 repressed renal fibrosis in vitro.

### 3.2 UUO-induced kidney injury ameliorated by ELA13 in mice

To determine whether ELA13 ameliorated renal injury and fibrosis in vivo, we established the mouse UUO experiment model with or without ELA13 treatment. As shown in Figs. 2a and 2b, the results of H&E staining revealed that the renal tubules were severely shrunken and the space between renal tubules was enlarged in the UUO model group. We also discovered through microscopic examination after Masson staining that the amounts of collagen and fibers in the kidney sections had increased rapidly. However, these pathological characteristics were significantly improved in mice treated with ELA13. To determine whether ELA13 ameliorated renal function, we measured levels of blood urea nitrogen (BUN) and serum creatinine. The results showed that BUN and serum creatinine contents were much higher in the UUO group than in the sham group, while they were much lower in the ELA13 treatment group (Figs. 2c and 2d). Thus, ELA13 ameliorated kidney injury in UUO mice.

### 3.3 Effects of ELA13 on kidney fibrosis in UUO-induced mice

After immunohistochemical analysis of Collagen I, fibronectin, and α-SMA, the quantitative data demonstrated that expression of these proteins was increased in UUO-induced mice, whereas the extent of protein deposition in the ELA13 group was inferior to that in the UUO group (Figs. 3a and 3b). Then we detected the messenger RNA (mRNA) expression of fibrosis markers by RT-PCR and western blot. As shown

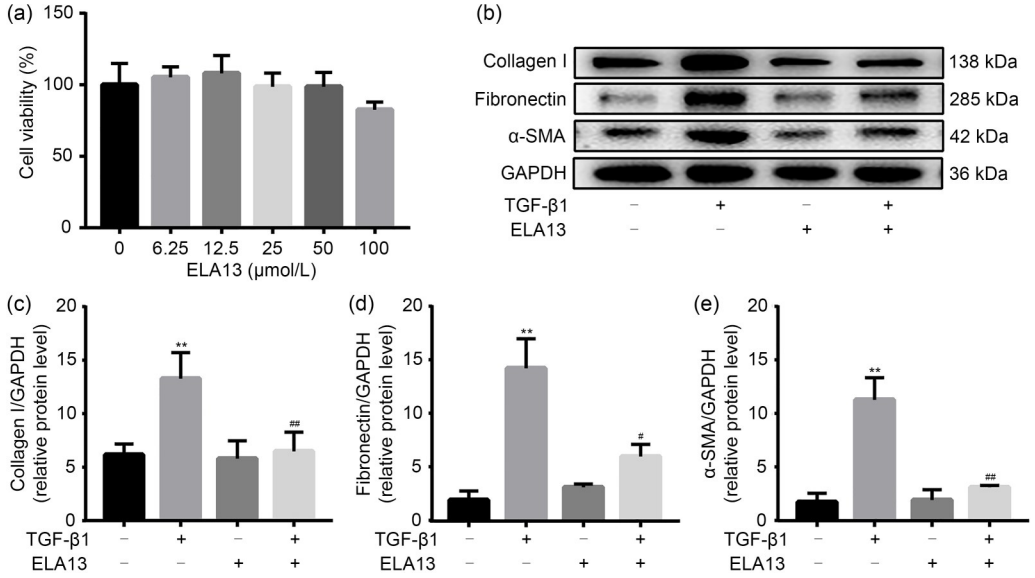


**Fig. 1 Effects of ELA13 on expression of renal fibrosis markers in TGF-β1-induced NRK-52E cells. (a) The toxicity of ELA13 in NRK-52E cells. (b) Expression of Collagen I, fibronectin, and α-SMA in different cell groups, as analyzed by western blot. (c–e) Mean quantitative results of proteins. The data are presented as mean±SD of three independent experiments. $^{**}P<0.01$, the TGF-β1 group vs. the control group; $^{\#}P<0.05$ and $^{\#\#}P<0.01$, the ELA13-treated group vs. the TGF-β1 group. TGF-β1: transforming growth factor-β1; α-SMA: α-smooth muscle actin; SD: standard deviation; GAPDH: glyceraldehyde-3-phosphate dehydrogenase.**

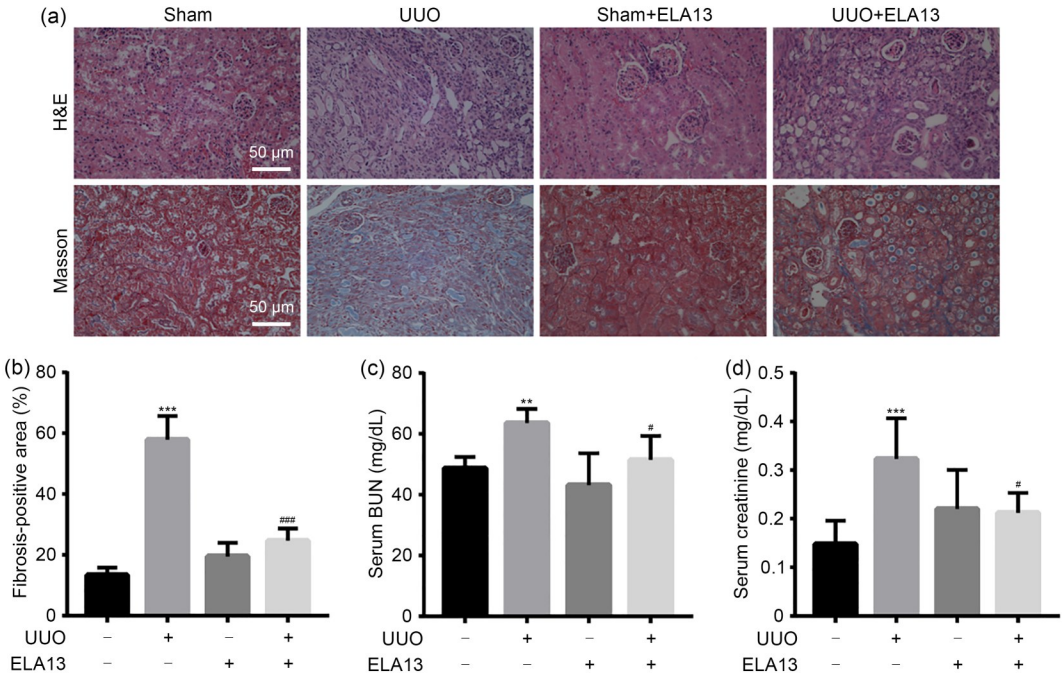


**Fig. 2 Interstitial fibrosis in UUO mice ameliorated by subcutaneously injecting ELA13. (a) H&E and Masson staining of renal slices. (b) Percentage of fibrosis areas. (c) Analysis of serum BUN. (d) Analysis of serum creatinine. All data are presented as mean±SD of three independent experiments. $^{**}P$<0.01 and $^{***}P$<0.001, the UUO group vs. the sham group; $^{\#}P$<0.05 and $^{\#\#\#}P$<0.001, the ELA13-treated group vs. the UUO group. UUO: unilateral ureteral occlusion; H&E: hematoxylin and eosin; BUN: blood urea nitrogen; SD: standard deviation.**

in Figs. 3c–3f, the mRNA expression of Collagen I, fibronectin, α-SMA, and TGF-β1 was greatly increased in mice induced by UUO, but decreased noticeably after ELA13 treatment. Parallel results were confirmed by western blot (Figs. 3g and 3h). All data demonstrated that treatment with ELA13 prevented fibrogenic effects in UUO-induced mice.

### 3.4 Effects of ELA13 on inflammation in UUO-induced mice

Since inflammation contributes to the process of tissue fibrosis and targeting inflammatory pathways may block the progression of kidney disease (Kanasaki et al., 2013), we next examined whether ELA13 inhibited kidney inflammation in our animal models. Expression of cluster of differentiation 68 (CD68), a typical inflammatory marker, was detected by immunohistochemistry. Compared with the sham group, protein deposition of CD68 in tissue sections subjected to UUO was sharply higher, while this phenomenon was remarkably mitigated in UUO mice treated with ELA13 (Fig. 4a). We investigated the mRNA levels of inflammatory markers IL-6, IL-1β, and MCP-1 by RT-PCR; the expression of inflammatory markers in the UUO group appeared to be higher than in the sham group, while the expression of UUO-induced elevated inflammatory factor was suppressed at the mRNA level by ELA13 treatment (Figs. 4b–4d). These results were also confirmed by western blot (Figs. 4e and 4f). Overall, ELA13 inhibited inflammation in mice with UUO-induced kidney fibrosis.

### 3.5 Effects of ELA13 on Smad and ERK signaling pathways in vivo and in vitro

Substantial evidence has shown that TGF-β/Smad and ERK signalings play key roles in fibrosis (Meng et al., 2015; Wojciechowski et al., 2018). We had found that ELA13 decreased TGF-β1 expression in UUO-induced renal fibrosis (Fig. 3). To investigate whether these two pathways were involved in the effects of ELA13, we first performed western blot analysis to detect related proteins in TGF-β1-induced NRK-52E cells, including p-Smad2/3 and p-ERK1/2. As expected, the levels of p-Smad2/3 and p-ERK1/2 induced by TGF-β1 were considerably increased, while they decreased after administration of ELA13 (Fig. 5a). Then, we carried out parallel experiments in the UUO model. We found that the relative phosphorylation levels of

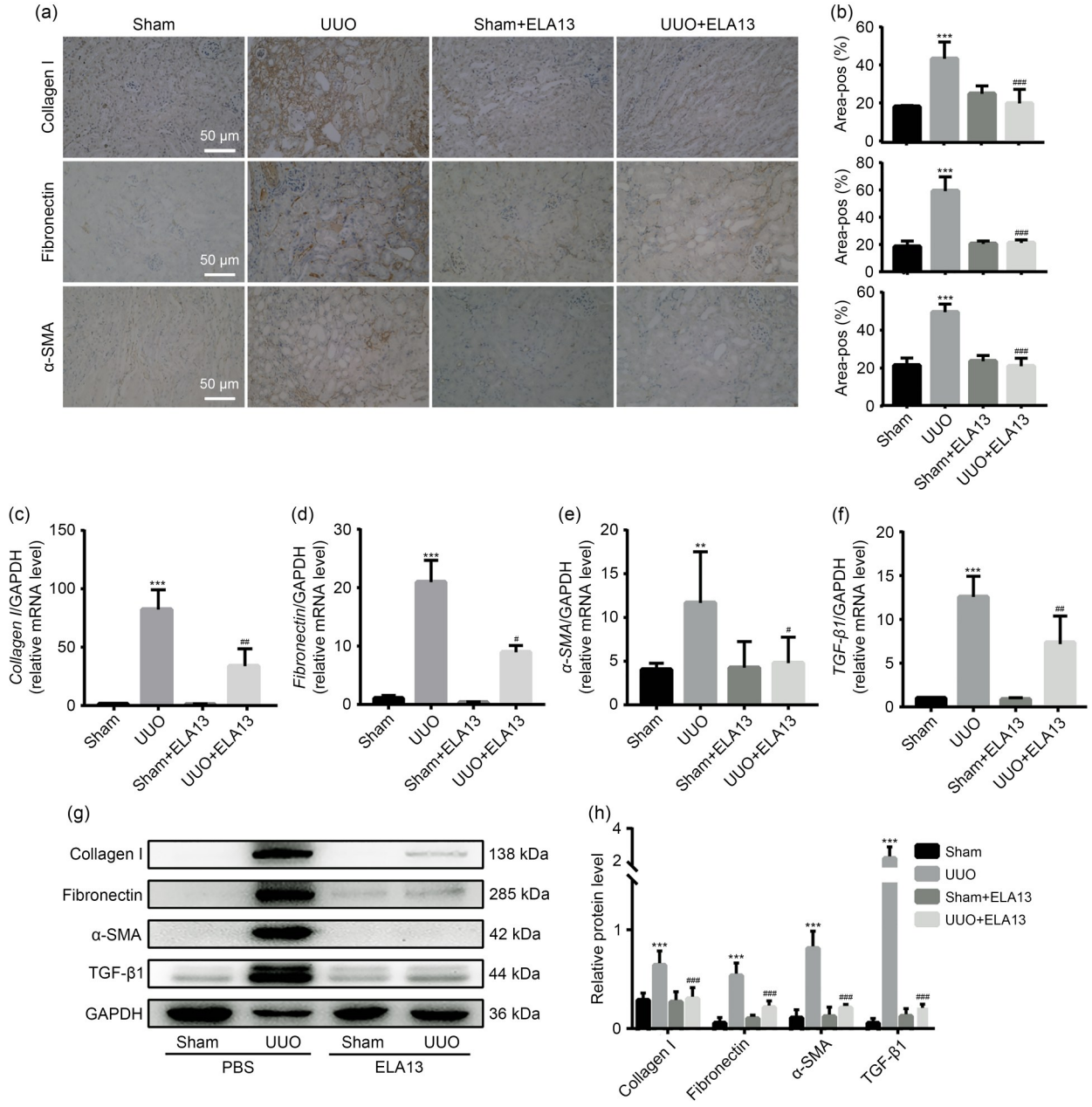


**Fig. 3 Effects of ELA13 on expression of kidney fibrosis markers in UUO-induced mice. (a) Immunohistochemistry staining for fibrosis markers Collagen I, fibronectin, and α-SMA in kidneys. (b) Quantification of immunohistochemistry for expression of these markers. (c–f) RT-PCR analyses of relative mRNA levels of *Collagen I*, *fibronectin*, *α-SMA*, and *TGF-β1* in different groups. (g) Representative western blots and densitometric quantitative results. (h) Expression of Collagen I, fibronectin, α-SMA, and TGF-β1 in different groups. The data are presented as mean±SD of three independent experiments. $^{**}P<0.01$ and $^{***}P<0.001$, the UUO group vs. the sham group; $^{\#}P<0.05$, $^{\#\#}P<0.01$, and $^{\#\#\#}P<0.001$, the ELA13-treated group vs. the UUO group. UUO: unilateral ureteral occlusion; α-SMA: α-smooth muscle actin; RT-PCR: real-time polymerase chain reaction; mRNA: messenger RNA; TGF-β1: transforming growth factor-β1; SD: standard deviation; Area-pos: area of positive staining; GAPDH: glyceraldehyde-3-phosphate dehydrogenase; PBS: phosphate-buffered saline.**

Smad2/3 and ERK1/2 were quite similar between the different groups. Interestingly, total Smad2/3 and ERK1/2 were obviously increased in the UUO group compared with the sham group, and ELA13 significantly attenuated total UUO-induced Smad2/3 and ERK1/2 levels (Fig. 5b). This implied that ELA13 was associated with Smad2/3 and ERK1/2 stability. To confirm the involvement of these signaling proteins in the

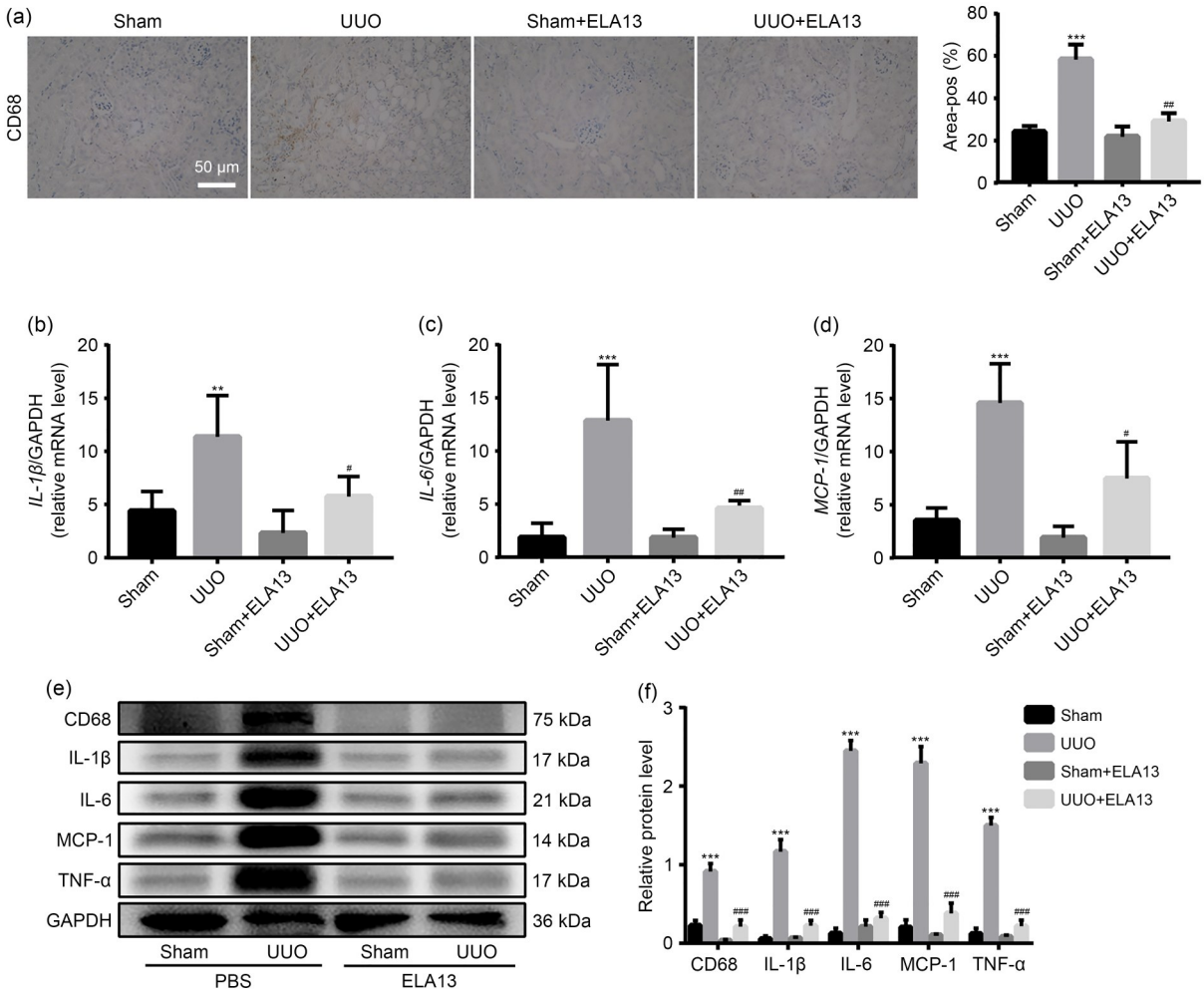


**Fig. 4 Effects of ELA13 on renal inflammation in UUO mice. (a) Immunohistochemistry staining for inflammatory marker CD68 in renal slices, and quantification of immunohistochemistry for CD68 expression. (b–d) RT-PCR analyses of relative mRNA levels of *IL-1β*, *IL-6*, and *MCP-1* in different mouse groups. (e, f) Western blot analysis and quantitative results of protein levels of CD68, IL-1β, IL-6, MCP-1, and TNF-α in different groups. The data are presented as mean± SD of three independent experiments. $^{**}P$<0.01 and $^{***}P$<0.001, the UUO group vs. the sham group; $^{\#}P$<0.05, $^{\#\#}P$<0.01, and $^{\#\#\#}P$<0.001, the ELA13-treated group vs. the UUO group. UUO: unilateral ureteral occlusion; CD68: cluster of differentiation 68; RT-PCR: real-time polymerase chain reaction; mRNA: messenger RNA; IL: interleukin; MCP-1: monocyte chemotactic protein-1; TNF-α: tumor necrosis factor-α; SD: standard deviation; Area-pos: area of positive staining; GAPDH: glyceraldehyde-3-phosphate dehydrogenase; PBS: phosphate-buffered saline.**

anti-fibrotic effects of ELA13, we used asiaticoside and U0126, which are proven inhibitors of Smad and ERK, respectively (Marampon et al., 2009; Huang et al., 2023). As shown in Figs. 5c and 5d, we observed that TGF-β stimulation increased expression of fibronectin and α-SMA; these fibrotic proteins were lower under ELA13 administration. Compared with ELA13 alone, the combination of ELA13 and the corresponding inhibitor significantly inhibited the expression of these fibrotic proteins. These results suggested that ELA13 inhibited renal fibrosis through the Smad and ERK pathways.

## 4 Discussion

In this study, we demonstrated that ELA13 significantly attenuated renal fibrosis in UUO-induced mice and TGF-β1-induced NRK-52E cells. UUO-induced mouse kidney fibrosis is characterized by dilated tubules, inflammatory-cell infiltration, interstitial fibrosis, and renal damage. Administration of ELA13 significantly improved renal function, interstitial fibrosis, and inflammation induced by UUO, suggesting a potent antifibrotic effect of ELA13. Furthermore, we showed

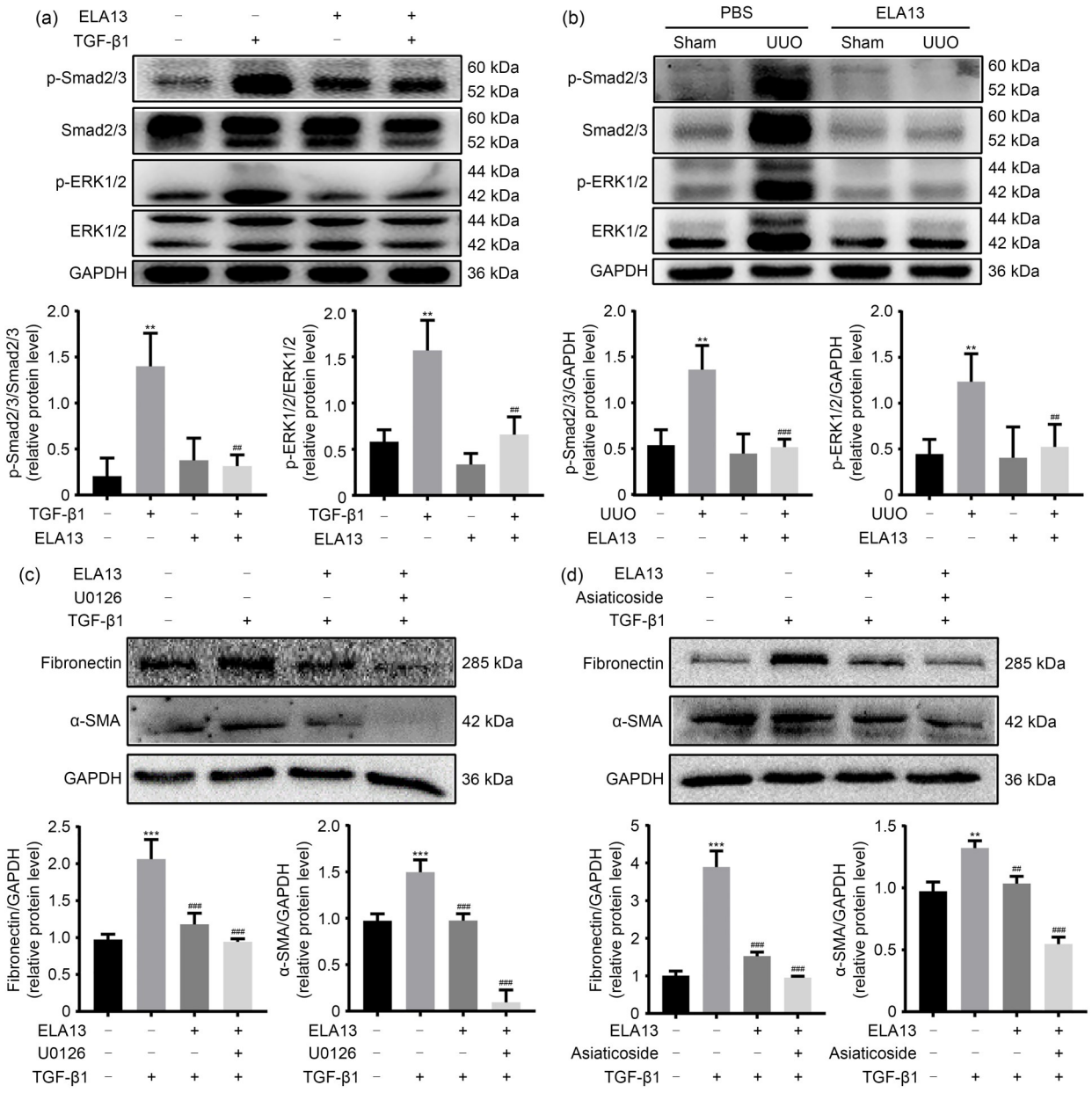


**Fig. 5 Effects of ELA13 on the Smad and ERK signaling pathways in vivo and in vitro. (a) Western blot analysis of the expression of p-Smad2/3, Smad2/3, p-ERK1/2, and ERK1/2 in vitro, and quantitative results of protein levels in different groups. (b) Western blot analysis of the expression of p-Smad2/3, Smad2/3, p-ERK1/2, and ERK1/2 in the UUO-induced model, and quantitative results of protein levels in different groups. (c, d) Western blot analysis of the expression of fibronectin and α-SMA under the action of ERK (c) and Smad (d) pathway inhibitors and ELA13 administration in vitro, and quantitative results of protein levels in different groups. The data are presented as mean±SD of three independent experiments. $^{**}P$<0.01 and $^{***}P$<0.001, the TGF-β1 group vs. the control group, the UUO group vs. the sham group; $^{\#\#}P$<0.01 and $^{\#\#\#}P$<0.001, the ELA13-treated group vs. the TGF-β1 group, the ELA13-treated group vs. the UUO group. Smad: small mother against decapentaplegic; ERK: extracellular signal-regulated kinase; p-: phosphorylated; UUO: unilateral ureteral occlusion; α-SMA: α-smooth muscle actin; SD: standard deviation; TGF-β1: transforming growth factor-β1; GAPDH: glyceraldehyde-3-phosphate dehydrogenase; PBS: phosphate-buffered saline.**

an inhibitory effect of ELA13 on the Smad and ERK pathways in vivo and in vitro (Fig. 6). This work may pave the way for the development of therapeutic strategies to address kidney fibrosis.

Both ELABELA and apelin are endogenous ligands of apelin receptor, a G-protein-coupled receptor that was found in 1993 (O'Dowd et al., 1993), but they are unrelated peptide ligands (Deng et al., 2015). Apelin

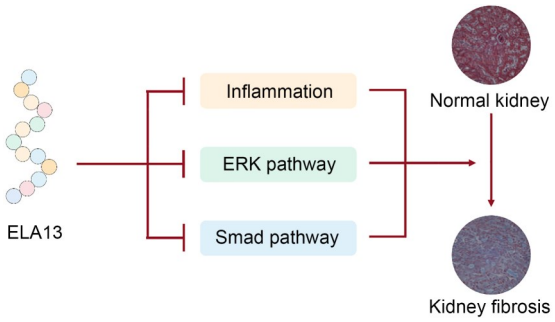


**Fig. 6 Schematic of ELA13 administration to attenuate kidney fibrosis.**

is widely expressed in various tissues (Lee et al., 2000; Wang et al., 2004; Boucher et al., 2005) and ELABELA is mainly expressed in the kidneys of mature mice (Deng et al., 2015). An early study from Mehal's group demonstrated that apelin inhibits renal tubular EMT in UUO mice by interfering with the TGF-β/Smads signaling pathway (Wang et al., 2014). Huang's Lab reported that ELABELA inhibits elevation of TGF-β1 and inflammation induced by ischemia-reperfusion (I/R) or hypoxia-reperfusion (H/R), without changing the level of total protein methylation (Chen et al., 2017). ELA11 not only inhibits inflammatory molecules in H/R-injured cells and I/R-injured kidney tissue, but also inhibits infiltration of macrophages in the latter (Chen et al., 2017). In the present study, the kidneys of UUO-induced mice expressed substantial levels of the fibrosis marker proteins Collagen I, fibronectin, and α-SMA. It is clear that ELA13, a conserved fragment of ELABELA in all vertebrates, has an anti-renal fibrosis effect in UUO-induced mice. The in vitro experiments also showed the inhibitory effect of ELA13 on the TGF-β1-induced fibrogenic response in cultured NRK-52E cells. TGF-β1 is a fibrogenic factor which can induce activation of the EMT in kidney tubular epithelial cells, as well as promoting synthesis of ECM protein (Grande et al., 2015).

The initial renal injury promotes the infiltration of immune cells and activated tubular cells can produce a series of local inflammatory factors, including TNF-α, IL-1β, and MCP-1, which in turn promote inflammatory response, fibroblast differentiation, and ECM accumulation, further leading to renal tubular atrophy and interstitial fibrosis (Wang et al., 2000; Noronha et al., 2002; Wada et al., 2004; Cheng et al., 2005; Crewe et al., 2017). Under normal circumstances, the level of chemokine expression in the kidney is very low, but under pathological conditions, it increases significantly. TNF-α and IL-1β are the main regulators of these chemokines, and can induce their expression through the nuclear factor-κB (NF-κB) signaling pathway (Seseke et al., 2004; Gilmore, 2006; Shen et al., 2016; Xue et al., 2016). In renal fibrosis, the function of IL-1β is mainly dependent on the fibrosis mechanism mediated by TGF-β (Maleszewska et al., 2013). Activation of the Smad2/3 signaling pathway mediated by TGF-β1 can also promote the expression of MCP-1/CC motif chemokine 2 (CCL2) (Wada et al., 2004; Tampe and Zeisberg, 2014), increase macrophage infiltration, and promote renal fibrosis. In our results, the immune-cell infiltration and chemokine expression in mice with UUO-induced fibrosis were significantly higher than those in normal mice; however, the expression of chemokines in mice treated with ELA13 was almost the same as that in normal mice, indicating that ELA13 had excellent anti-inflammatory effects in mice with UUO-induced fibrosis. Nevertheless, it is currently unclear how ELA13 inhibits inflammation, and this definitely warrants further investigation.

TGF-β binds to its type II receptor, and then causes the activation of several intracellular signaling pathways, including Smad2/3, signal transducer and activator of transcription 3 (STAT3), and ERK1/2, which activate fibroblasts and lead to the accumulation of ECM in the relevant tissue (Xu et al., 2012; Sun et al., 2014; Chen et al., 2019). The Smad-dependent signaling pathway is the canonical signal pathway of the TGF-β signal, which plays a fatal role in renal fibrosis. TGF-β1 first binds to the type II receptor on the cell surface to form a heterodimer complex; then the phosphorylated complex binds to a type I receptor to form a tetramer which is activated by phosphorylation. The phosphorylated tetramer activates the Smad2/3 complex and prompts Smad2/3 to form a new complex with Smad4. The new complex enters the nucleus and directly binds to the Smad protein combinatorial element on DNA to regulate the expression of target genes (Zhang et al., 2010; Meng et al., 2016). A string of noncanonical TGF-β pathways has been identified, such as the MAPKs, in particular ERK1/2 (Hartsough and Mulder, 1995), a member of the MAPK family. Once stimulated, ERK can translocate to the nucleus to activate transcriptional factors that regulate cell growth and differentiation. Emerging studies have indicated that the ERK1/2 signaling pathway is important for EMT,

a biological transformation of epithelial cells into mesenchymal phenotypic cells, which eventually promotes the pathobiology of fibrosis (Lu et al., 2017; Schinner et al., 2017). We found that the phosphorylated expression of Smad2/3 and ERK1/2 is apparently inhibited under the administration of ELA13 in TGF-β1-induced NRK-52E cells. However, there do not appear to be any significant differences in the relative phosphorylation levels of Smad2/3 and ERK1/2 in vivo. ELA13 significantly attenuates total UUO-induced Smad2/3 and ERK1/2 levels. These results are in line with a recent published study by Geng et al. (2020), who showed that ganoderic acid markedly decreases total Smad in a UUO model. Another work by Yang et al. (2020) also reveals that the level of total ERKs is significantly enhanced in UUO kidneys. These findings suggest that UUO may enhance Smad2/3 and ERK1/2 stability, and that ELA13 may be associated with protein degradation. In general, our results suggest that ELA13 has a therapeutic effect on obstructive renal fibrosis by inhibiting the Smad and ERK pathways. In addition, the detailed mechanism of ELA13 in kidney fibrosis needs to be elucidated by future research.

In summary, these original observations demonstrate the potent anti-fibrotic activity of ELA13 in UUO-induced mice and TGF-β1-induced NRK-52E cells by inhibiting the Smad and ERK pathways. These results provide novel insight into the role of ELABELA and suggest that ELA13 may be a promising new candidate for renal fibrosis treatment.

## Data availability statement

The data presented in this study are available from the corresponding author upon reasonable request.

## Acknowledgments

This work was supported by the Zhejiang Provincial Natural Science Foundation of China (No. LD22H310004), the National Natural Science Foundation of China (No. 82204492), the CAMS Innovation Fund for Medical Sciences (CIFMS) (No. 2019-I2M-5-074), the Medical Innovation and Development Project of Lanzhou University (No. lzuyxcx-2022-156), and the Scientific Research Foundation of Zhejiang Sci-Tech University (No. 21042100-Y), China.

## Author contributions

Caiyun FU supervised the studies and provided financial support. Zhibin YAN and Ying SHI designed the research and drafted the original manuscript. Runling YANG and Jijun XUE edited and revised manuscript. All authors have read and approved the content of the manuscript, and therefore, have full access to all the data in the study and take responsibility for the integrity and security of the data.

## Compliance with ethics guidelines

Caiyu FU is a Young Scientist Committee Member for *Journal of Zhejiang University-SCIENCE B (Biomedicine & Biotechnology)* and was not involved in the editorial review or the decision to publish this article. Zhibin YAN, Ying SHI, Runling YANG, Jijun XUE, and Caiyun FU declare that they have no conflict of interest.

All institutional and national guidelines for the care and use of laboratory animals were followed. The experimental protocols were performed under the Guidelines for the Care and Use of Laboratory Animals and approved by the Laboratory Animals Use Committee of the Zhejiang Sci-Tech University (No. 20210315-01), Hangzhou, China.

## References

Akter T, Rahman MA, Moni A, et al., 2021. Prospects for protective potential of *Moringa oleifera* against kidney diseases. *Plants*, 10(12):2818. https://doi.org/10.3390/plants10122818

Boucher J, Masri B, Daviaud D, et al., 2005. Apelin, a newly identified adipokine up-regulated by insulin and obesity. *Endocrinology*, 146(4):1764-1771. https://doi.org/10.1210/en.2004-1427

Chen H, Wang L, Wang WJ, et al., 2017. ELABELA and an ELABELA fragment protect against AKI. *J Am Soc Nephrol*, 28(9):2694-2707. https://doi.org/10.1681/ASN.2016111210

Chen W, Yuan H, Cao WM, et al., 2019. Blocking interleukin-6 trans-signaling protects against renal fibrosis by suppressing STAT3 activation. *Theranostics*, 9(14):3980-3991. https://doi.org/10.7150/thno.32352

Cheng JF, Encarnacion MMD, Warner GM, et al., 2005. TGF-$\beta_1$ stimulates monocyte chemoattractant protein-1 expression in mesangial cells through a phosphodiesterase isoenzyme 4-dependent process. *Am J Physiol Cell Physiol*, 289(4):C959-C970. https://doi.org/10.1152/ajpcell.00153.2005

Crewe C, An YA, Scherer PE, 2017. The ominous triad of adipose tissue dysfunction: inflammation, fibrosis, and impaired angiogenesis. *J Clin Invest*, 127(1):74-82. https://doi.org/10.1172/JCI88883

Deng C, Chen HD, Yang N, et al., 2015. Apela regulates fluid homeostasis by binding to the APJ receptor to activate Gi signaling. *J Biol Chem*, 290(30):18261-18268. https://doi.org/10.1074/jbc.M115.648238

Ding Y, Kim SL, Lee SY, et al., 2014. Autophagy regulates TGF-$\beta$ expression and suppresses kidney fibrosis induced by unilateral ureteral obstruction. *J Am Soc Nephrol*, 25(12):2835-2846. https://doi.org/10.1681/ASN.2013101068

el Agha E, Kramann R, Schneider RK, et al., 2017. Mesenchymal stem cells in fibrotic disease. *Cell Stem Cell*,

21(2):166-177.
https://doi.org/10.1016/j.stem.2017.07.011

El-Ghoul B, Elie C, Sqalli T, et al., 2009. Nonprogressive kidney dysfunction and outcomes in older adults with chronic kidney disease. *J Am Geriatr Soc*, 57(12):2217-2223.
https://doi.org/10.1111/j.1532-5415.2009.02561.x

Geng XQ, Ma A, He JZ, et al., 2020. Ganoderic acid hinders renal fibrosis via suppressing the TGF-β/Smad and MAPK signaling pathways. *Acta Pharmacol Sin*, 41(5):670-677.
https://doi.org/10.1038/s41401-019-0324-7

Gilmore TD, 2006. Introduction to NF-*κ*B: players, pathways, perspectives. *Oncogene*, 25(51):6680-6684.
https://doi.org/10.1038/sj.onc.1209954

Grande MT, Sánchez-Laorden B, López-Blau C, et al., 2015. Snail1-induced partial epithelial-to-mesenchymal transition drives renal fibrosis in mice and can be targeted to reverse established disease. *Nat Med*, 21(9):989-997.
https://doi.org/10.1038/nm.3901

Harris RC, Neilson EG, 2006. Toward a unified theory of renal progression. *Annu Rev Med*, 57(1):365-380.
https://doi.org/10.1146/annurev.med.57.121304.131342

Hartsough MT, Mulder KM, 1995. Transforming growth factor β activation of $p44^{mapk}$ in proliferating cultures of epithelial cells. *J Biol Chem*, 270(13):7117-7124.
https://doi.org/10.1074/jbc.270.13.7117

Huang XM, Jia ZQ, Li XY, et al., 2023. *Asiaticoside* hampers epithelial–mesenchymal transition by promoting PPARG expression and suppressing P2RX7-mediated TGF-β/Smad signaling in triple-negative breast cancer. *Phytother Res*, 37(5):1771-1786.
https://doi.org/10.1002/ptr.7692

Ji XL, Wang HL, Wu ZJ, et al., 2018. Specific Inhibitor of Smad3 (SIS3) attenuates fibrosis, apoptosis, and inflammation in unilateral ureteral obstruction kidneys by inhibition of transforming growth factor β (TGF-β)/Smad3 signaling. *Med Sci Monit*, 24:1633-1641.
https://doi.org/10.12659/msm.909236

Jiang S, Li T, Yang Z, et al., 2017. AMPK orchestrates an elaborate cascade protecting tissue from fibrosis and aging. *Ageing Res Rev*, 38:18-27.
https://doi.org/10.1016/j.arr.2017.07.001

Kanasaki K, Taduri G, Koya D, 2013. Diabetic nephropathy: the role of inflammation in fibroblast activation and kidney fibrosis. *Front Endocrinol (Lausanne)*, 4:7.
https://doi.org/10.3389/fendo.2013.00007

Kanda H, Hirasaki Y, Iida T, et al., 2017. Perioperative management of patients with end-stage renal disease. *J Cardiothorac Vasc Anesth*, 31(6):2251-2267.
https://doi.org/10.1053/j.jvca.2017.04.019

Korpal M, Kang Y, 2010. Targeting the transforming growth factor-β signalling pathway in metastatic cancer. *Eur J Cancer*, 46(7):1232-1240.
https://doi.org/10.1016/j.ejca.2010.02.040

Kovacs RJ, Maldonado G, Azaro A, et al., 2015. Cardiac Safety of TGF-β receptor I kinase inhibitor LY2157299 monohydrate in cancer patients in a first-in-human dose study. *Cardiovasc Toxicol*, 15(4):309-323.
https://doi.org/10.1007/s12012-014-9297-4

Lan HY, 2011. Diverse roles of TGF-β/Smads in renal fibrosis and inflammation. *Int J Biol Sci*, 7(7):1056-1067.
https://doi.org/10.7150/ijbs.7.1056

Lee DK, Cheng R, Nguyen T, et al., 2000. Characterization of apelin, the ligand for the APJ receptor. *J Neurochem*, 74(1):34-41.
https://doi.org/10.1046/j.1471-4159.2000.0740034.x

Li Z, Zhou LL, Wang YP, et al., 2017. (Pro)renin receptor is an amplifier of Wnt/β-catenin signaling in kidney injury and fibrosis. *J Am Soc Nephrol*, 28(8):2393-2408.
https://doi.org/10.1681/ASN.2016070811

López-Hernández FJ, López-Novoa JM, 2012. Role of TGF-β in chronic kidney disease: an integration of tubular, glomerular and vascular effects. *Cell Tissue Res*, 347(1):141-154.
https://doi.org/10.1007/s00441-011-1275-6

Lu JH, Zhong YZ, Lin ZC, et al., 2017. Baicalin alleviates radiation-induced epithelial-mesenchymal transition of primary type II alveolar epithelial cells via TGF-β and ERK/GSK3β signaling pathways. *Biomed Pharmacother*, 95:1219-1224.
https://doi.org/10.1016/j.biopha.2017.09.037

Maleszewska M, Moonen JRAJ, Huijkman N, et al., 2013. IL-1β and TGFβ2 synergistically induce endothelial to mesenchymal transition in an NFκB-dependent manner. *Immunobiology*, 218(4):443-454.
https://doi.org/10.1016/j.imbio.2012.05.026

Marampon F, Bossi G, Ciccarelli C, et al., 2009. MEK/ERK inhibitor U0126 affects *in vitro* and *in vivo* growth of embryonal rhabdomyosarcoma. *Mol Cancer Ther*, 8(3):543-551.
https://doi.org/10.1158/1535-7163.MCT-08-0570

Meng J, Li LM, Zhao Y, et al., 2016. MicroRNA-196a/b mitigate renal fibrosis by targeting TGF-*β* receptor 2. *J Am Soc Nephrol*, 27(10):3006-3021.
https://doi.org/10.1681/ASN.2015040422

Meng XM, Nikolic-Paterson DJ, Lan HY, 2014. Inflammatory processes in renal fibrosis. *Nat Rev Nephrol*, 10(9):493-503.
https://doi.org/10.1038/nrneph.2014.114

Meng XM, Tang PMK, Li J, et al., 2015. TGF-β/Smad signaling in renal fibrosis. *Front Physiol*, 6:82.
https://doi.org/10.3389/fphys.2015.00082

Noronha IL, Fujihara CK, Zatz R, 2002. The inflammatory component in progressive renal disease—are interventions possible? *Nephrol Dial Transplant*, 17(3):363-368.
https://doi.org/10.1093/ndt/17.3.363

Nutter FH, Haylor JL, Khwaja A, 2015. Inhibiting ERK activation with CI-1040 leads to compensatory upregulation of alternate MAPKs and plasminogen activator inhibitor-1 following subtotal nephrectomy with no impact on kidney fibrosis. *PLoS ONE*, 10(9):e0137321.
https://doi.org/10.1371/journal.pone.0137321

O'Dowd BF, Heiber M, Chan A, et al., 1993. A human gene that shows identity with the gene encoding the angiotensin receptor is located on chromosome 11. *Gene*, 136(1-2):355-360.
https://doi.org/10.1016/0378-1119(93)90495-o

Rahman MH, Biswas P, Dey D, et al., 2022. An in-silico identification of potential flavonoids against kidney fibrosis targeting TGFβR-1. *Life*, 12(11):1764. https://doi.org/10.3390/life12111764

Rahman MA, Akter S, Dorotea D, et al., 2022. Renoprotective potentials of small molecule natural products targeting mitochondrial dysfunction. *Front Pharmacol*, 13:925993. https://doi.org/10.3389/fphar.2022.925993

Reichman-Fried M, Raz E, 2014. Small proteins, big roles: the signaling protein Apela extends the complexity of developmental pathways in the early zebrafish embryo. *Bioessays*, 36(8):741-745. https://doi.org/10.1002/bies.201400048

Romagnani P, Kalluri R, 2009. Possible mechanisms of kidney repair. *Fibrogenesis Tissue Repair*, 2:3. https://doi.org/10.1186/1755-1536-2-3

Schinner E, Wetzl V, Schramm A, et al., 2017. Inhibition of the TGFβ signalling pathway by cGMP and cGMP-dependent kinase I in renal fibrosis. *FEBS Open Bio*, 7(4):550-561. https://doi.org/10.1002/2211-5463.12202

Schreiber CA, Holditch S, Generous A, et al., 2016. Sustained ELABELA gene therapy in high-salt diet-induced hypertensive rats. *Curr Gene Therapy*, 16(5):349-360.

Seseke F, Thelen P, Ringert RH, 2004. Characterization of an animal model of spontaneous congenital unilateral obstructive uropathy by cDNA microarray analysis. *Eur Urol*, 45(3):374-381. https://doi.org/10.1016/j.eururo.2003.10.010

Shen WC, Liang CJ, Huang TM, et al., 2016. Indoxyl sulfate enhances IL-1β-induced E-selectin expression in endothelial cells in acute kidney injury by the ROS/MAPKs/NFκB/AP-1 pathway. *Arch Toxicol*, 90(11):2779-2792. https://doi.org/10.1007/s00204-015-1652-0

Sun SR, Ning XX, Zhai Y, et al., 2014. Egr-1 mediates chronic hypoxia-induced renal interstitial fibrosis via the PKC/ERK pathway. *Am J Nephrol*, 39(5):436-448. https://doi.org/10.1159/000362249

Tampe D, Zeisberg M, 2014. Potential approaches to reverse or repair renal fibrosis. *Nat Rev Nephrol*, 10(4):226-237. https://doi.org/10.1038/nrneph.2014.14

Tanaka S, Tanaka T, Nangaku M, 2015. Hypoxia and dysregulated angiogenesis in kidney disease. *Kidney Dis*, 1(1):80-89. https://doi.org/10.1159/000381515

Wada T, Furuichi K, Sakai N, et al., 2004. Gene therapy via blockade of monocyte chemoattractant protein-1 for renal fibrosis. *J Am Soc Nephrol*, 15(4):940-948. https://doi.org/10.1097/01.asn.0000120371.09769.80

Wang GY, Anini Y, Wei W, et al., 2004. Apelin, a new enteric peptide: localization in the gastrointestinal tract, ontogeny, and stimulation of gastric cell proliferation and of cholecystokinin secretion. *Endocrinology*, 145(3):1342-1348. https://doi.org/10.1210/en.2003-1116

Wang LY, Diao ZL, Zhang DL, et al., 2014. The regulatory peptide apelin: a novel inhibitor of renal interstitial fibrosis. *Amino Acids*, 46(12):2693-2704. https://doi.org/10.1007/s00726-014-1826-8

Wang SN, LaPage J, Hirschberg R, 2000. Role of glomerular ultrafiltration of growth factors in progressive interstitial fibrosis in diabetic nephropathy. *Kidney Int*, 57(3):1002-1014. https://doi.org/10.1046/j.1523-1755.2000.00928.x

Wang Z, Yu DZ, Wang MQ, et al., 2015. Elabela-apelin receptor signaling pathway is functional in mammalian systems. *Sci Rep*, 5:8170. https://doi.org/10.1038/srep08170

Wojciechowski MC, Shu DY, Lovicu FJ, 2018. ERK1/2-dependent gene expression contributing to TGFβ-induced lens EMT. *Curr Eye Res*, 43(8):986-997. https://doi.org/10.1080/02713683.2018.1464193

Xu T, Wang NS, Fu LL, et al., 2012. Celecoxib inhibits growth of human autosomal dominant polycystic kidney cyst-lining epithelial cells through the VEGF/Raf/MAPK/ERK signaling pathway. *Mol Biol Rep*, 39(7):7743-7753. https://doi.org/10.1007/s11033-012-1611-2

Xue HY, Yuan L, Cao YJ, et al., 2016. Resveratrol ameliorates renal injury in spontaneously hypertensive rats by inhibiting renal micro-inflammation. *Biosci Rep*, 36(3):e00339. https://doi.org/10.1042/BSR20160035

Yan ZB, Cheng XR, Wang T, et al., 2022. Therapeutic potential for targeting Annexin A1 in fibrotic diseases. *Genes Dis*, 9(6):1493-1505. https://doi.org/10.1016/j.gendis.2022.05.038

Yang L, Guo J, Yu N, et al., 2020. Tocilizumab mimotope alleviates kidney injury and fibrosis by inhibiting IL-6 signaling and ferroptosis in UUO model. *Life Sci*, 261:118487. https://doi.org/10.1016/j.lfs.2020.118487

Zeisberg M, Neilson EG, 2010. Mechanisms of tubulointerstitial fibrosis. *J Am Soc Nephrol*, 21(11):1819-1834. https://doi.org/10.1681/ASN.2010080793

Zhang DS, Sun L, Xian W, et al., 2010. Low-dose paclitaxel ameliorates renal fibrosis in rat UUO model by inhibition of TGF-β/Smad activity. *Lab Invest*, 90(3):436-447. https://doi.org/10.1038/labinvest.2009.149

Zhang YH, Wang SY, Liu SM, et al., 2015. Role of Smad signaling in kidney disease. *Int Urol Nephrol*, 47(12):1965-1975. https://doi.org/10.1007/s11255-015-1115-9

Zhang YX, Wang YW, Luo MY, et al., 2019. Elabela protects against podocyte injury in mice with streptozocin-induced diabetes by associating with the PI3K/Akt/mTOR pathway. *Peptides*, 114:29-37. https://doi.org/10.1016/j.peptides.2019.04.005

Zhuang ZH, Tong MK, Clarke R, et al., 2022. Probability of chronic kidney disease and associated risk factors in Chinese adults: a cross-sectional study of 9 million Chinese adults in the Meinian Onehealth screening survey. *Clin Kidney J*, 15(12):2228-2236. https://doi.org/10.1093/ckj/sfac176